Climate Models Indicate Compensating Effects between Anthropogenic Greenhouse Gases and Aerosols on the 2022 Central Andes Spring Drought

Jonghun Kam,[a,f] Seung-Ki Min,[a,f] Byeong-Hee Kim,[a] Yeon-Hee Kim,[a] Leandro B. Diaz,[b,c,d] and Jong-Seong Kug,[a] and Rokjin Park[e]

CMIP6 simulations showed a weak human contribution to 2022-like Central Andes spring droughts, due to compensating impacts between anthropogenic greenhouse gases and aerosols.

AFFILIATIONS: [a] Division of Environmental Science and Engineering, POSTECH, Pohang, 37673, South Korea; [b] Facultad de Ciencias Exactasy Naturales, Departamento de Ciencias de la Atmósfera y los Océanos, Universidad de Buenos Aires, Buenos Aires, Argentina; [c] Centro de Investigaciones del Mar y la Atmósfera, CONICET–Universidad de Buenos Aires, Buenos Aires, Argentina; [d] Instituto Franco-Argentino de Estudios sobre el Clima y sus Impactos–IRL 3351–CNRS–CONICET–IRD, Universidad de Buenos Aires, Buenos Aires, Argentina; [e] School of Earth and Environmental Sciences, Seoul National University, Seoul, South Korea; [f] Institute for Convergence Research and Education in Advanced Technology, Yonsei University, Seoul, South Korea

DOI: 10.1175/BAMS-D-23-0241.1

CORRESPONDING AUTHOR: Jonghun Kam, jhkam@postech.ac.kr

Supplemental information related to this paper is available at the Journals Online website: https://doi.org/10.1175/BAMS-D-23-0241.s1.

Manuscript received 18 September 2023, in final form 8 January 2024, accepted 12 February 2024

The Central Andes is a semiarid mountainous region (above 4000 m MSL) with a short period of precipitation between late spring and early summer (Sanabria et al. 2014). The Central Andes includes southern Peru, western Bolivia, and northern Chile and is vulnerable to hydroclimatic extremes, such as droughts and floods (Mortensen et al. 2018; Giorgi et al. 2018; Potter et al. 2023). According to the WMO annual report (WMO 2023), the 2022 rainfall deficits over the Central Andes ranged from 20% to 60% and were mostly associated with the La Niña condition. The austral spring (September–November) of 2022 was the driest (beyond the 2σ range) over the Central Andes since 1951 (Fig. 1a). The extremeness of the drought in 2022 was from interannual variability imposed onto this negative trend through weak northeastward moisture transports in 2022 (blue arrows in Fig. 1b). This drying trend was found in previous studies (Vera et al. 2019; Morales et al. 2023).

According to the U.S. Department of Agriculture,[1] the austral spring is a planting season of major crops over the

[1] https://ipad.fas.usda.gov/ogamaps/cropcalendar.aspx.

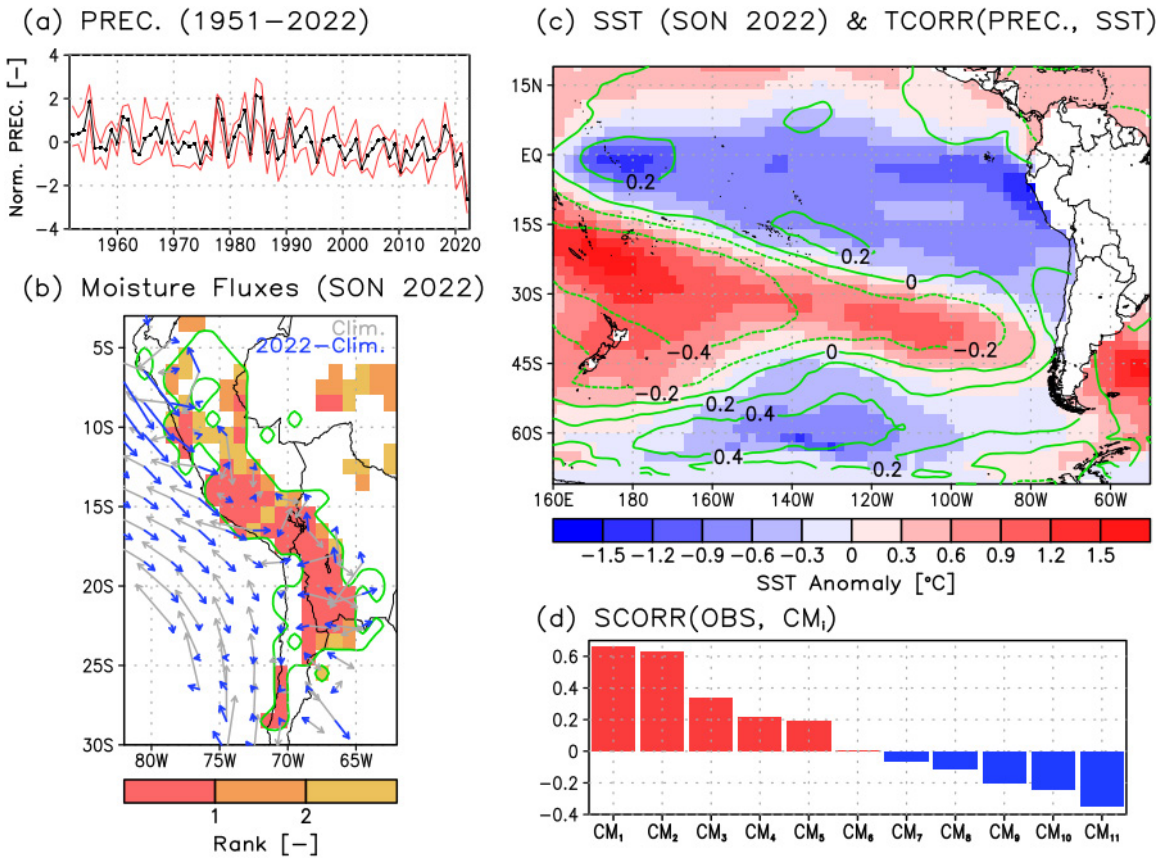

Fig. 1. Atmospheric and oceanic conditions of the Central Andes in the spring of 2022. (a) Black and red lines depict the averages and the maximum/minimum values of nPREC among the five observed data products, respectively. (b) Background colors depict the first (red), second (orange), and third (yellow) lowest precipitation since 1951, and gray and blue arrows depict the climatological moisture fluxes over 1951–2022 and moisture flux anomalies in 2022, respectively. (c) Background colors and contour lines depict sea surface temperature anomalies relative to the climatology and the temporal correlations of SSTs with nPREC over 1951–2022, respectively. (d) Bars depict the pattern correlation coefficients of the observed and simulated temporal correlation maps of SST teleconnections [contour lines in (c) and see Fig. S1] across the 11 CMIP6 models [CMi on the y axis in (d) is depicted in Table S1].

Central Andes. The Cconchaccota lagoon in Peru has been a vital water source for communities. It was totally dried out in the austral spring of 2022, threatening 3000 local communities (Briceño 2022). According to the International Federation of Red Cross and Red Crescent Societies report,[2] Bolivia presented the national drought response plans in November 2022, providing assistance to 53 municipalities in eight out of nine departments. The 2022 drought in Bolivia provided a favorable condition for forest fires, which resulted in extensive wildfires over 2.7 million hectares in 2023 (Arriaza 2023).

[2] https://adore.ifrc.org/Download.aspx?FileId=744525.

Variability of the regional precipitation over the Central Andes is associated with orographic uplift along the eastern hill side and meridional wind convergence at high elevations (Lenters and Cook 1995). Increasing anthropogenic greenhouse gas emissions contributed to a positive trend of 200-hPa zonal wind anomalies and associated precipitation deficits over the Central Andes, but with a relatively weak magnitude compared with internal variability (Neukom et al. 2015; Vera et al. 2019).

Regional climate model projections showed that surface warming increases the water vapor holding capacity of air and thus intensifies hydroclimatic variability, resulting in more frequent intense precipitation and severe droughts over the Central Andes (Potter et al. 2023).

However, these previous studies about the attribution, mechanism, and future change of the Central Andes hydrological extremes have focused on the austral summer season due to its importance on the annual total of the regional precipitation. Aerosol optical depth (AOD) of the Central Andes has a strong seasonality with a peak season between August and October (Pérez-Ramírez et al. 2017). While GHG-driven surface warming plays a role in melting the glaciers over the Andes, increases in deposition of anthropogenic aerosols, such as black carbon from biomass burning and atmospheric particulates from local mining activities, affect the regional climate (Csavina et al. 2012; Cereceda-Balic et al. 2022; Bonilla et al. 2023). The role of these anthropogenic aerosols in spring droughts over the Central Andes still remains unknown.

This study aims to assess the anthropogenic contribution to the likelihood of 2022-like austral spring droughts over the Central Andes, using historical (HIST; natural + greenhouse gas + aerosol), natural-only (NAT; solar + volcanic), anthropogenic GHG-only (GHG), and anthropogenic aerosol-only (AER; black carbon, sulfur dioxide, atmospheric particulates, etc.) forcing simulations of 11 phase 6 of the Coupled Model Intercomparison Project (CMIP6) models (Eyring et al. 2016). The findings of this study will advance our knowledge about the relative importance of anthropogenic individual forcings on Central Andes spring droughts and provide an actionable information to develop region-specific strategies for climate change mitigation and adaptation.

Data and methods

In this study, column integrated moisture fluxes were calculated from monthly meridional and zonal winds and specific humidity from the land product of the fifth major global reanalysis produced by the European Centre for Medium-Range Weather Forecasts (ECMWF) (ERA5-Land; Muñoz-Sabater et al. 2021). The regional averages of austral spring precipitation (PREC) over the Central Andes (4°–25°S of the west side of the Andes) were calculated from five observational data products: NOAA/CIRES–DOE Twentieth Century Reanalysis (20C), version 3 (1836–2015; Slivinski et al. 2019); CRU TS v4.07 (Harris et al. 2020); GPCC (Schneider et al. 2017); GPCP (1979–2022; Adler et al. 2012); and ERA5-Land. The study period was chosen over 1951–2022 because of a large difference of the regional averages between the CRU and GPCC data before 1951. This study used the Extended Reconstructed Sea Surface Temperature (ERSST), version 5, dataset (Huang et al. 2017) to compute the Niño-3.4 index (5°N–5°S, 120°–170°W).

This study used simulated PREC and SST data from 68, 58, 50, and 57 ensemble runs of 11 CMIP6 models with HIST-, NAT-, GHG-, and AER-forcing, respectively. These ensemble runs of the 11 models were selected based on the availability of multiple ensemble members (≥3 ensemble members of HIST-, NAT-, GHG-, and AER-forcing runs). The HIST-forcing runs (ended in 2014) were extended up to 2022 using the corresponding ensemble members of the shared socioeconomic pathway (SSP) 2.45 scenario runs, considering their similar future radiative forcing over 2015–22 (O'Neill et al. 2016). Details of the ensemble runs of each model were provided in Table S1 (in the online supplemental material). For the consistent spatial scale for analysis, a bilinear method was used to interpolate the model data onto the observed grids (1°) and then the regional averages of SST and PREC over the Niño-3.4 region (5°N–5°S, 170°–120°W) and Central Andes and were calculated, respectively. The linearly detrended Niño-3.4 regional averages (Niño-3.4) were used to identify years with a cold phase of the tropical Pacific Ocean in the corresponding model, like the year of 2022.

The regional averages of PREC from individual forcing runs were normalized by the 2003–22 means and standard deviations from the HIST-forcing runs (nPREC). The contributions of HIST-, NAT-, GHG-, and AER-forcing to the observed nPREC were examined during the 2022 and 2010 springs (first and second driest springs since 1951; Fig. 1b). The nPREC values are

similar to the 3-month standardized precipitation index, except for fitting to the Gaussian distribution function. Here, a drought year was defined when the observed nPREC value was less than the 2010 value (–1.2), as the 2022 value (–2.37) is rare in CMIP6 model simulations. This threshold value was used to compute the drought frequency from all the experiment forcing runs. In this study, drought frequency was computed by the ratio of the number of the drought years to the preceding 20 years.

Here the last 20-yr segment of austral spring nPREC (2003–22) were used to estimate the contribution of each forcing to the observed anomalies in 2022, following the methods of previous studies (Kam et al. 2021, 2022). In this study, the 20-yr segments (2001–20) of the NAT-, GHG-, AER-forcing ensemble runs were used because most of the CMIP6 individual forcing runs were ended in 2020. We constructed the 95% uncertainty range of each forcing's contribution by randomly sampling the 20-yr segment of the HIST runs 68 times with replacement, that is, the total sample size is 1360 (20-yr segment × 68 ensemble runs). This 20-yr segment was weighted by each model's contribution to the total ensemble runs. For example, the 20-yr segment for CESM2 was randomly sampled with replacement 3 times among three available ensemble runs. This 20-yr segment random sampling procedure was repeated 1000 times (bootstrapping).

This study used the austral spring averages of the observed (daily) and simulated (monthly) AOD at 550 nm from the MODIS Daily L3 Products[3] (MOD08_D3; 2000–22) and the 11 CMIP6 models, respectively (Ramachandran et al. 2022). Fewer ensemble members of the 11 CMIP6 models are available for AOD than PREC and SST (see Table S1). The simulated AOD data were regridded at the 1° resolution. Then, the regional averages of the observed and simulated AODs over the study region were calculated over 2000–22 and 1951–2022, respectively.

[3] https://ladsweb.modaps.eosdis.nasa.gov/archive/allData/61/MOD08_D3/.

The discrete probability distributions of nPREC for HIST-, NAT-, GHG-, and AER-forcing runs (P_H, P_N, P_G, and P_A) were constructed, and then the probabilities of exceeding the observed 2022 (first driest since 1951) and 2010 (second driest) values were calculated for all the cases and negative Niño-3.4 cases to check whether the anthropogenic impact has been affected by La Niña-like phases. The probability ratios (PRs) were calculated for $P_{\mathrm{HIST}}/P_{\mathrm{NAT}}$, $P_{\mathrm{GHG}}/P_{\mathrm{NAT}}$, and $P_{\mathrm{AER}}/P_{\mathrm{NAT}}$. The 95% uncertainty range of PRs was estimated using the 1000 bootstrapped samples of the 20-yr segments.

Results

The observational data showed the first and second lowest nPREC for 2022 and 2010, respectively (Fig. 1a). The nPREC values for 2022 and 2010 ranged from –3.25 (CRU) to –2.37 (ERA5) and from –1.6 (GPCP) to –1.2 (CRU), respectively. The observational data showed a wide range in the mid-1980s and late-1990s, indicating a significant uncertainty of the data sources. For a conservative analysis (the least observed deficit), the observed nPREC values, –2.37 and –1.2, were used for 2022 and 2010, respectively. In the austral spring of 2022, the Niño-3.4 index showed a cold phase, which is well known as the last year of triple-dip La Niña (Fig. 1c; Jones 2022). Historically, the cold Niño-3.4 phase was associated with precipitation deficits over the study region, but with a limited explanatory power (<20%; $r_{\max} < 0.5$). The CMIP6 models showed diverse SST teleconnections with the Central Andes precipitation compared to the observed SST teleconnections (green contour lines in Fig. 1c). The pattern correlation between the SST-PREC correlation maps from the observed and the CMIP6 models (the multiensemble mean of each model) ranged from −0.38 to 0.6 (Fig. 1d), indicating significant uncertainties of the CMIP6 models in reproducing SST teleconnections for this region (Fig. S1). This tendency might be spring-specific, which is needed to study further for other seasons.

Observed drought frequency showed an increasing trend since 2010 (Fig. 2a). Multiensemble model means (MMMs; the average of the ensemble averages of each model, that is, one vote for one model) of the CMIP6 models showed an increasing trend only from the AER-forcing runs. The MMMs of nPREC showed a decreasing (moderately decreasing) trend of nPREC from the AER-forcing (HIST-forcing) runs (Fig. 2b). This result indicated a possible impact of the AER-forcing on decreased nPREC over the Central Andes.

The AER-forcing made the mean precipitation more negative but the GHG-forcing increased the probability of more extreme positive precipitation, indicating the asymmetry in the probability distributions from the AER- and GHG-forcing runs (the right tail of the distribution). This asymmetry is important for changes in the risk of extreme precipitation deficits. This asymmetry is important for changes in the risk of extreme precipitation deficits. These impacts of the AER- and GHG-forcings were compensated in the HIST-forcing runs. The PR values of

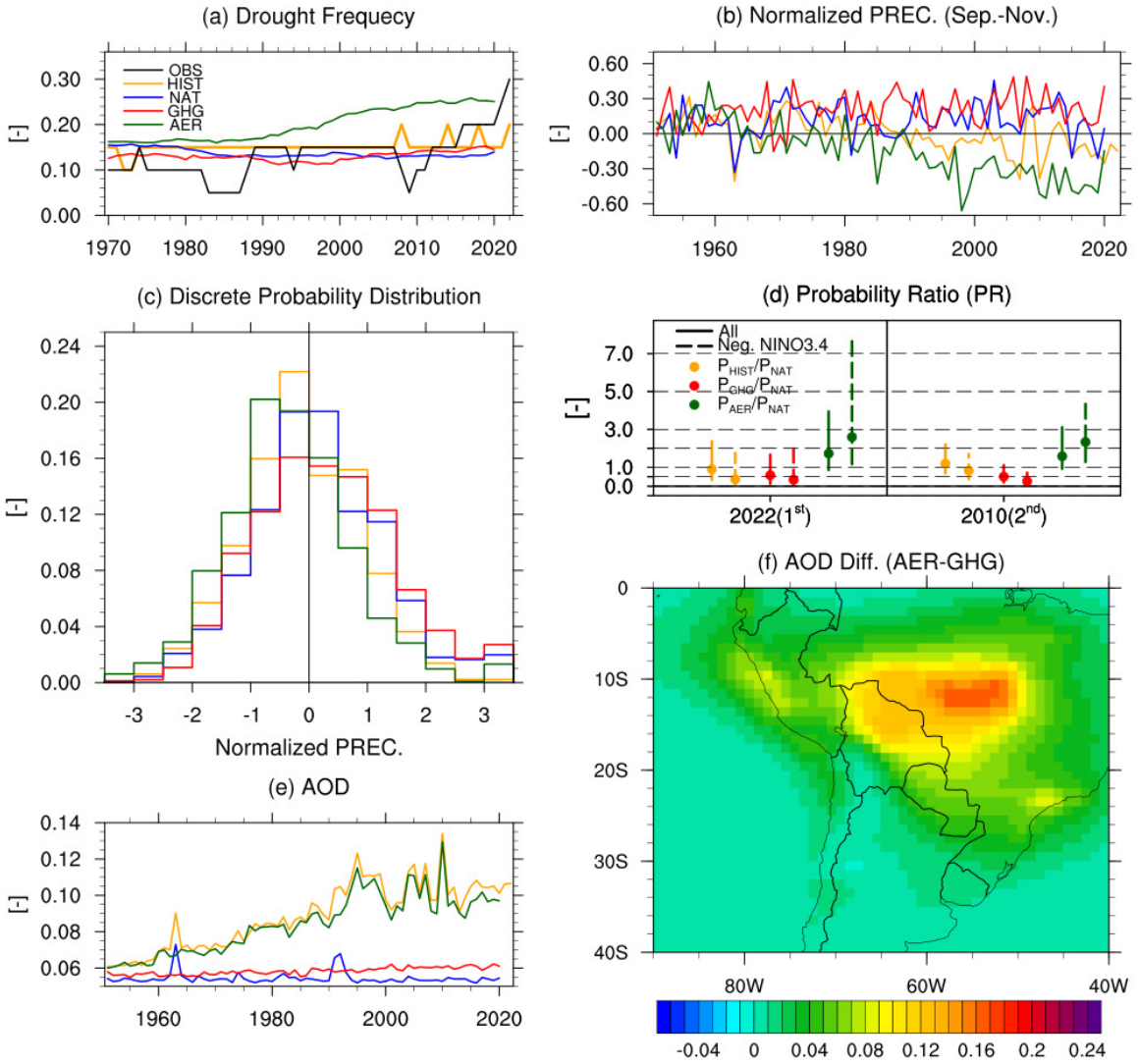

Fig. 2. (a) Observed and simulated drought frequencies and (b) simulated normalized precipitation from the HIST-, GHG-, AER-, and NAT-forcing runs. (c) Lines depict the discrete probability distribution of the 20-yr segment bootstrapped samples from the HIST- (orange line), NAT- (blue), GHG- (red), AER-forcing (green) runs. (d) Circles depict the me-dian ratios of exceeding probability of 2022- and 2010-like nPREC (first and second lowest), and error bars depict their 95% uncertainty range. (e) Orange, blue, red, and green lines depict the regional average of the simulated AOD values over the Central Andes by the HIST-, NAT-, GHG-, and AER-forcing ensemble runs. (f) Background colors depict the averages of the AOD differences between the AER- and GHG-forcing ensemble runs over 2000–20.

P_H/P_N, P_G/P_N, and P_A/P_N for the observed nPREC in 2022 (2010) from the 20-yr segment are 0.9 (1.2), 0.6 (0.5), and 1.7 (1.6) (Fig. 2d).

The contribution of AER-forcing to 2022/10-like spring droughts was marginal, which was compensated with GHG forcing-driven effect on increasing precipitation. Given the negative Niño-3.4 phases, the values of P_H/P_N, P_G/P_N, and P_A/P_N of 2022 (2010)-like spring droughts were 0.37 (0.82), 0.33 (0.26), and 2.6 (2.3). This result implied that a negative Niño-3.4 phase can amplify the impact of both forcings, resulting in the overwhelming impact of the GHG-forcing in the HIST-forcing (AER + GHG) simulations. Assessment of the combined impact of AER- and GHG-forcing in various SST conditions and their SST–teleconnection diversity should be further investigated (Rugenstein et al. 2023).

Over 1951–2022, the increasing trends of observed and simulated AODs were likely a favorable condition for reduced rainfall over the Central Andes (Fig. 2e). The NAT-forcing runs showed an increase of AODs in early 1960s and 1990s, which was related to the 1963/64 Agung and 1991 Pinatubo 1991 eruptions. This result indicated that eruption-associated increased aerosols were smaller than the human-activity-associated aerosols over the Central Andes. The MMMs of the AODs of the AER-forcing runs showed a large difference over the Central Andes and western Amazon (due to biomass burning and atmospheric particulates) from those of the GHG-forcing on average (Fig. 2f), which was consistent with the observed AOD patterns from the MODIS product (Fig. S2).

In summary, the 2022 Central Andes spring was the driest on record since 1951. Based on the selected 11 CMIP6 simulations, AER-forcing has likely contributed to the increased probability of such spring droughts, by a factor of 1.7. The cold sea surface conditions with AER-forcing can increase it up to 2.6 but with a wide 95% uncertainty range. In contrast, the GHG-forcing has likely contributed to the decreased probability of 2022-like spring droughts by the shift toward a wetter condition. In this study, CMIP6 individual forcing runs were used to assess the contribution of increasing anthropogenic greenhouse gases and aerosols to 2022-like droughts, but not the abrupt increase of AODs observed in 2022. Furthermore, the compensating impact of the AER- and GHG-forcing resulted in no conclusive anthropogenic attribution to 2022-like droughts over the Central Andes. A poor representation of SST teleconnections with Central Andes spring precipitation in CMIP6 models suggests a possible underestimation of the increased probability of a 2022-like drought. Another potential uncertainty source of the current CMIP6 models was a poor representation of complex terrains of CMIP6 models (Fig. S3). High-resolution regional climate model simulations over the Central Andes should be designed for detection and attribution assessments, in addition to climate projection (Llopart et al. 2020), to provide actionable information for climate change mitigation and adaptation policies.

Acknowledgments. We thank the CMIP6 project for making available the CMIP6 data and the CRU and RIHMI-WDC for providing observational temperature and precipitation datasets. J. K. is partially supported by the NRF Basic Research Program (NRF-2020R1A4A1018818). L. D. acknowledges funding from Agencia I+D+i, PICT-2020-SERIEA-I-INVI-00540, and CONICET PIBAA 28720210100758CO.

References

Adler, R. F., G. Gu, and G. Huffman, 2012: Estimating climatological bias errors for the Global Precipitation Climatology Project (GPCP). *J. Appl. Meteor. Climatol.*, **51**, 84–99, https://doi.org/10.1175/JAMC-D-11-052.1.

Arriaza, M., 2023: Amid a severe drought, slash-and-burn fuels controversy in Bolivia. EL PAÍS, 23 December, https://english.elpais.com/international/2023-11-03/amid-a-severe-drought-slash-and-burn-fuels-controversy-in-bolivia.html.

Bonilla, E. X., and Coauthors, 2023: Contribution of biomass burning to black carbon dep-osition on Andean glaciers: Consequences for radiative forcing. *Environ. Res. Lett.*, **18**, 024031, https://doi.org/10.1088/1748-9326/acb371.

Briceño, F., 2022: Lagoon dries up as drought grips Peru's southern Andes. AP News, https://apnews.com/article/science-mountains-peru-caribbean-3d132d36842004884bd87902d1221744.

Cereceda-Balic, F., M. F. Ruggeri, V. Vidal, L. Ruiz, and J. S. Fu, 2022: Understanding the role of anthropogenic emissions in glaciers retreat in the central Andes of Chile. *Environ. Res.*, **214**, 113756, https://doi.org/10.1016/j.envres.2022.113756.

Csavina, J., J. Field, M. P. Taylor, S. Gao, A. Landázuri, E. A. Betterton, and A. E. Sáez, 2012: A review on the importance of metals and metalloids in atmospheric dust and aerosol from mining operations. *Sci. Total Environ.*, **433**, 58–73, https://doi.org/10.1016/j.scitotenv.2012.06.013.

Eyring, V., S. Bony, G. A. Meehl, C. A. Senior, B. Stevens, R. J. Stouffer, and K. E. Tay-lor, 2016: Overview of the Coupled Model Intercomparison Project Phase 6 (CMIP6) exper-imental design and organization. *Geosci. Model Dev.*, **9**, 1937–1958, https://doi.org/10.5194/gmd-9-1937-2016.

Giorgi, F., E. Coppola, and F. Raffaele, 2018: Threatening levels of cumulative stress due to hydroclimatic extremes in the 21st century. *npj Climate Atmos. Sci.*, **1**, 18, https://doi.org/10.1038/s41612-018-0028-6.

Harris, I., T. J. Osborn, P. Jones, and D. Lister, 2020: Version 4 of the CRU TS monthly high-resolution gridded multivariate climate dataset. *Sci. Data*, **7**, 109, https://doi.org/10.1038/s41597-020-0453-3.

Huang, B., and Coauthors, 2017: NOAA Extended Reconstructed Sea Surface Tempera-ture (ERSST), version 5. NOAA NCEI, accessed 16 February 2023, https://doi.org/10.7289/V5T72FNM.

Jones, N., 2022: Rare 'triple' La Niña climate event looks likely—What does the future hold? *Nature*, **607**, 21, https://doi.org/10.1038/d41586-022-01668-1.

Kam, J., S.-K. Min, P. Wolski, and J.-S. Kug, 2021: CMIP6 model-based assessment of an-thropogenic influence on the long sustained Western Cape drought over 2015–19. *Bull. Amer. Meteor. Soc.*, **102**, S45–S50, https://doi.org/10.1175/BAMS-D-20-0159.1.

——, ——, C.-K. Park, B.-H. Kim, and J.-S. Kug, 2022: Human contribution to 2020/21-like persistent Iran meteorological droughts. *Bull. Amer. Meteor. Soc.*, **103**, E2930–E2936, https://doi.org/10.1175/BAMS-D-22-0149.1.

Lenters, J. D., and K. H. Cook, 1995: Simulation and diagnosis of the regional summertime precipitation climatology of South America. *J. Climate*, **8**, 2988–3005, https://doi.org/10.1175/1520-0442(1995)008<2988:SADOTR>2.0.CO;2.

Llopart, M., M. Simões Reboita, and R. Porfírio da Rocha, 2020: Assessment of multi-model climate projections of water resources over South America CORDEX domain. *Climate Dyn.*, **54**, 99–116, https://doi.org/10.1007/s00382-019-04990-z.

Morales, M. S., and Coauthors, 2023: Drought increase since the mid-20th century in the northern South American Altiplano revealed by a 389-year precipitation record. *Climate Past*, **19**, 457–476, https://doi.org/10.5194/cp-19-457-2023.

Mortensen, E., S. Wu, M. Notaro, S. Vavrus, R. Montgomery, J. De Piérola, C. Sánchez, and P. Block, 2018: Regression-based season-ahead drought prediction for southern Peru conditioned on large-scale climate variables. *Hydrol. Earth Syst. Sci.*, **22**, 287–303, https://doi.org/10.5194/hess-22-287-2018.

Muñoz-Sabater, J., and Coauthors, 2021: ERA5-Land: A state-of-the-art global reanalysis dataset for land applications. *Earth Syst. Sci. Data*, **13**, 4349–4383, https://doi.org/10.5194/essd-13-4349-2021.

Neukom, R., M. Rohrer, P. Calanca, N. Salzmann, C. Huggel, D. Acuña, D. A. Christie, and M. S. Morales, 2015: Facing unprecedented drying of the Central Andes? Precipitation variability over the period AD 1000–2100. *Environ. Res. Lett.*, **10**, 084017, https://doi.org/10.1088/1748-9326/10/8/084017.

O'Neill, B. C., and Coauthors, 2016: The Scenario Model Intercomparison Project (ScenarioMIP) for CMIP6. *Geosci. Model Dev.*, **9**, 3461–3482, https://doi.org/10.5194/gmd-9-3461-2016.

Pérez-Ramírez, D., and Coauthors, 2017: Multi year aerosol characterization in the tropical Andes and in adjacent Amazonia using AERONET measurements. *Atmos. Environ.*, **166**, 412–432, https://doi.org/10.1016/j.atmosenv.2017.07.037.

Potter, E. R., and Coauthors, 2023: A future of extreme precipitation and droughts in the Peruvian Andes. *npj Climate Atmos. Sci.*, **6**, 96, https://doi.org/10.1038/s41612-023-00409-z.

Ramachandran, S., M. Rupakheti, and R. Cherian, 2022: Insights into recent aerosol trends over Asia from observations and CMIP6 simulations. *Sci. Total Environ.*, **807**, 150756, https://doi.org/10.1016/j.scitotenv.2021.150756.

Rugenstein, M., S. Dhame, D. Olonscheck, R. J. Wills, M. Watanabe, and R. Seager, 2023: Connecting the SST pattern problem and the hot model problem. *Geophys. Res. Lett.*, **50**, e2023GL105488, https://doi.org/10.1029/2023GL105488.

Sanabria, J., P. Calanca, C. Alarcón, and G. Canchari, 2014: Potential impacts of early twenty-first century changes in temperature and precipitation on rainfed annual crops in the Central Andes of Peru. *Reg. Environ. Change*, **14**, 1533–1548, https://doi.org/10.1007/s10113-014-0595-y.

Schneider, U., P. Finger, A. Meyer-Christoffer, E. Rustemeier, M. Ziese, and A. Becker, 2017: Evaluating the Hydrological Cycle over Land Using the Newly-Corrected Precipitation Climatology from the Global Precipitation Climatology Centre (GPCC). *Atmos.*, 8, 52, https://doi.org/10.3390/atmos8030052.

Slivinski, L. C., and Coauthors, 2019: Towards a more reliable historical reanalysis: Im-provements for version 3 of the Twentieth Century Reanalysis system. *Quart. J. Roy. Meteor. Soc.*, **145**, 2876–2908, https://doi.org/10.1002/qj.3598.

Vera, C. S., L. B. Díaz, and R. I. Saurral, 2019: Influence of anthropogenically-forced global warming and natural climate variability in the rainfall changes observed over the South American Altiplano. *Front. Environ. Sci.*, **7**, 87, https://doi.org/10.3389/fenvs.2019.00087.

WMO, 2023: State of the climate in Latin America and the Caribbean 2022. WMO-1322, 39 pp., https://library.wmo.int/doc_num.php?explnum_id=11701.